Original Article – Evaluative Research

Induction of multinucleated giant cells in response to small sized bovine bone substitute (Bio-Oss™) results in an enhanced early implantation bed vascularization

Access this article online
Website: www.amsjournal.com
DOI: 10.4103/2231-0746.147106
Quick Response Code:

M. Barbeck[1,2], S. E. Udeabor[2], J. Lorenz[2], A. Kubesch[1,2], J. Choukroun[3], R. A. Sader[2], C. J. Kirkpatrick[1], S. Ghanaati[1,2]

[1]Department of Oral, Cranio-Maxillofacial and Facial Plastic Surgery, Medical Center of the Goethe University Frankfurt, Germany, [2]REPAIR Laboratory, Institute of Pathology, University Medical Center of the Johannes Gutenberg University, Langenbeckstrasse 1, D-55131 Mainz, Germany , [3]Pain Clinic, 49 rue Gioffredo, 06000 Nice, France

Address for correspondence:
Dr. Shahram Ghanaati, Department of Oral, Cranio-Maxillofacial and Facial Plastic Surgery, Medical Center of the Goethe University Frankfurt, Theodor-Stein-Kai 7, D - 60596 Frankfurt am Main, Germany.
E-mail: shahram.ghanaati@kgu.de

ABSTRACT

Purpose: The host tissue reaction to the xenogeneic bone substitute Bio-Oss™ (Geistlich Biomaterials, Wolhousen, Switzerland) was investigated focusing on the participating inflammatory cells and implantation bed vascularization. **Materials and Methods:** Bio-Oss™ was implanted subcutaneously into CD1 mice for up to 60 days and analyzed by means of specialized histological and histomorphometrical techniques after explantation. **Results:** Bio-Oss™ induced within the first 15 days an early high vascularization combined with a marked presence of multinucleated giant cells. The latter cells were associated mainly with the smaller sized granules within the implantation bed. Toward the end of the study the number of multinucleated giant cells decreased while the tissue reaction to the larger granules was mainly mononuclear. **Conclusion:** The results of the present study showed that smaller xenogeneic bone substitute granules induce multinucleated giant cells, whereas the larger-sized ones became integrated within the implantation bed by means of a mononuclear cell-triggered granulation tissue. Obviously, the presence of multinucleated giant cells within biomaterial implantation beds is not only related to the type of synthetic bone substitute material, but also to the granule size of the "natural-based" xenogeneic bone substitute material.

Keywords: Bio-Oss, multinucleated giant cells, vascularization, xenogeneic bone substitute

INTRODUCTION

The use of bone grafts and their substitutes in clinical practice is on the increase. Many surgical procedures in the field of oral and maxillofacial surgery, implantology, periodontology, endodontics, among others require the use of bone grafts in different forms.[1] To be ideal, these bone substitutes must possess the following properties: Osteoinduction, osteogenesis, osteointegration and osteoconduction.[2,3] Even though, autogenous bone graft possesses all these properties, thus making it the most effective bone graft material, it is still not an ideal bone graft because of its limited availability, prolonged surgery time, donor site morbidity, wound complications, and chronic pain.[2-4]

Allografts also have all the characteristics of autografts with the exception of osteogenesis due to the processing that they must undergo. Some are subjected to lyophilization and demineralization, which leaves them more brittle, while others undergo biomechanical alteration with the loss of compressive, bending and torsional strength.[1] The processing chemicals may also be potentially toxic and there is always the risk of disease transmission, especially HIV and hepatitis.[1,3] These materials are also not available in some countries because of social and religious concerns and where available, are generally very expensive.[3]

Heterografts or xenografts on the other hand consist of bone minerals derived from animals and have been processed to

remove the organic component, thus eliminating the risk of immunogenic reactions and disease transmission.[1] Xenografts derived from natural bone sources have been extensively investigated, in particular cancellous bovine bone, due to its similarity to human bone. Bio-Oss™ (Geistlich Biomaterials, Wolhousen, Switzerland) is a deproteinized bovine bone material, which is currently one of the best researched biomaterials. It is sintered at a high-temperature and subjected to a sequence of other processing and sterilization methods leaving only its mineral content.[5]

Various *in vivo* studies have shown Bio-Oss™ to be highly biocompatible, stable and to have a long-term efficacy.[6-9] It has also been shown to be present in the augmentation site years after implantation,[7] and so has the capacity to form a stable foundation for subsequent implantations. This has made it suitable for use in sinus lift, mandibular and maxillary bone augmentations, guided bone regeneration, and a host of other surgical applications.[6-8]

Alloplastic bone substitute materials (hydroxyapatite [HA]), and α- and β-tricalcium phosphate (α- and β-TCP) have been shown in previous studies to attract multinucleated giant cells after implantation, although at different rates.[10-12] These cells are thought to be responsible for the degradation of the bone substitute materials and at the same time induce vascularization by releasing vascular endothelial growth factor (VEGF) and other biologically active compounds, such as chemokines.[10] The number of these multinucleated giant cells at the implantation bed varies, depending on the physicochemical structure of the biomaterials, as previously demonstrated by our research group.[3,10]

Our research group has also shown differing rates of foreign body giant cells (FBGCs) on implantation of different granule sizes of nanocrystalline HA and β-TCP in the subcutaneous tissue of Wistar rats.[13,14] A mixture of these two synthetic biomaterials also seemed to combine the stability of HA with the greater multinucleated giant cell attraction of β-TCP.[15]

Bio-Oss™ has been extensively studied in terms of its degradation and clinical applications as described earlier.[6,7,12] However, little is known about the participating cells and the cellular mechanisms taking place in the initial integration and degradation process of the bone substitute material. This is important, as it will further improve decision-making for the suitability of the bone substitute in various surgical bone augmentation procedures.[1]

Therefore, this study was aimed to investigate the cellular reaction to the implantation of a bovine bone substitute (Bio-Oss™) in a well-established subcutaneous implantation bed model. Special interest was in the analysis and categorization of the participating inflammatory cells and the level of induced vascularization.

MATERIALS AND METHODS

Bone substitute

The analyzed bone substitute Bio-Oss™ is a xenogeneic biomaterial, which originates from the cancellous parts of bovine bone of veterinary inspected donor animals.[16,17] The extracted bone tissue is processed via heat and chemical treatment to remove the organic tissue components such as connective tissue, remnants of bone marrow and bone protein components and then subjected to a final ɣ-radiation.[17] During the purification process, the tissue initially undergoes a high-temperature purification process at 300°C for more than 15 h, followed by an additional thorough cleansing via alkaline solution.[17,18] Therefore, only the mineral bone components in their natural micro- and ultrastructure are assumed to remain, which is very similar to the structure of the human bone.[19] The trabecular architecture has a pore size ranging from 300 to 1500 µm, a porosity of 70-75% and an internal surface area of 97 m^2/g.[20] The studied bone substitute is in granular form with sizes ranging from 0.25 to 1 mm for the small granules, while larger granules range from 1 to 2 mm.

Extensive analyses have also been conducted to ensure the purity of this bone substitute material, that is, to prevent the risk of disease transmission.[19]

Microscopic evaluation of biomaterials microstructure

For purpose of microscopic evaluation of microstructure and purification control, the bone substitute was decalcified in 10% tris-buffered ethylenediaminetetraacetic acid (EDTA) (Carl Roth, Karlsruhe, Germany) at 37°C for 10 days and embedded in paraffin prior to sectioning. Subsequently, sections of 4 µm were cut with a microtome (Leica, Wetzlar, Germany) and special histochemical staining reactions for evaluation of the structure and contents with special focus on connective tissue components were made as follows: The first section was stained with hematoxylin and eosin (H and E), while the subsequent sections were stained with Movat's Pentachrome, Azan, and Giemsa. In addition, a histochemical staining method for the detection of tartrate-resistant acid phosphatase (TRAP)-positive osteoclastic cells was applied as previously described.[10,13-15]

In vivo animal study

Experimental design of the subcutaneous implantation model in CD1 mice

Animal experiments were performed after approval by the Committee on the Use of Live Animals in Teaching and Research of the State of Rhineland-Palatinate, Germany. For conduction of the present *in vivo* study, 35 female 6-8 weeks old CD1 mice (Charles River Laboratories, Germany) were used after a standardized study protocol, which included animal accommodation under standard conditions (water *ad libitum*, regular rat pellet [Laboratory Rodent Chow, Altromin, Germany], artificial light with a night and day cycle) at the *in vivo* Laboratory Animal Unit of the Institute of Pathology, Johannes Gutenberg University of Mainz, Germany.[10,13-15,21] Furthermore, the study protocol included the random division of the animals to the following three experimental groups: 20 animals were used for implantation of Bio-Oss™. Four animals each were allocated for subcutaneous implantation of the bone substitute to the standardized study time points that is, 3, 10 and 15, 30 and 60 days, according to a previously described method.[10,13-15] A second group of 15 animals, that is, three animals for each of the above-mentioned study time points, was used as control for analysis of the tissue reactions related to the operation without biomaterial insertion.

Subcutaneous implantation

The subcutaneous implantation was conducted after a standardized and published protocol.[10,13-15,21] Briefly, after intraperitoneal anesthesia with 10 ml of ketamine (50 mg/ml) in combination with 1.6 ml of 2% xylazine, 60 mg of the bone substitute material were implanted under sterile conditions. An incision was made in the rostral area of the interscapular region and the biomaterial incorporated under the skin in the prepared pocket. Wound adaption was obtained by stitching with Prolene 6.0 (Ethicon, Somerville, NJ, USA).

Tissue preparation of the implantation area

After sacrifice of the animals, the biomaterial and the peri-implant tissue were explanted and processed as previously described.[10,13-15,21] The explants at the respective study time points were fixed in 4% formalin for 24 h. Each explanted sample of the 35 animals was further cut in three segments that is, the left margin, the right margin, and the central part. In the next step, the biopsies were decalcified in 10% tris-buffered EDTA at 37°C for 30 days and afterwards dehydrated in a series of increasing alcohol concentrations followed by xylol exposure. Subsequently, the samples were embedded in paraffin and cut in sections of 4 µm with a microtome.

Histochemical staining methods

The first section of every explant was used for standard staining with H and E, whereas two consecutive sections were used for staining with Movat's Pentachrome and Azan. The third section was used for identification of osteoclast-like cells by staining for TRAP according to a previously described method.[10,13-15]

Immunohistochemical staining methods

For immunohistochemical detection of murine vessels and macrophages, four further sections were used as previously described.[21] Following the quenching of endogenous peroxidase activity using Dual Endogenous Enzyme Block, Dako S2003 (Dako, Glostrup, Denmark), a monoclonal anti-mouse CD31 antibody Dianova DIA 310, Clone SZ31 (Dianova Hamburg, Germany, diluted 1:35) was used to detect vascular endothelial cells. A DAKO REAL™ EnVision™ detection system HRP-DAB Dako, K5007 (Dako, Glostrup, Denmark) which contains a link-antibody (Rabbit-Anti-Rat Dako P0450 [Dako, Glostrup, Denmark, 1:175]) was used to visualize these cells. As negative controls, immunohistological stains were performed on each control section in the absence of the primary antibody. For visualization by light microscopy, the sections used for immunohistology were counterstained with hematoxylin.

Qualitative histological analysis

Histopathological examination was performed to determine the tissue-biomaterial-interactions and the extent of early and late inflammatory response caused by the biomaterial. Two independent investigators conducted the evaluation, using a conventional diagnostic microscope (Eclipse 80i, Nikon, Tokyo, Japan) to evaluate the total implantation bed and the peri-implant tissue of each specimen. The inflammatory response was described using the following parameters as previously described:[10,13-15,21] Integration pattern of the biomaterial granules, fibrosis, hemorrhage, necrosis, vascularization and the presence of neutrophils, lymphocytes, plasma cells, macrophages, multinucleated giant cells, and TRAP-positive osteoclast-like cells.

Quantitative histological analysis (histomorphometry)

The histomorphometric analysis was performed after a standardized and established protocol.[10,13-15,21] According to the manufacturer's instructions, the NIS-elements AR software (version 4.10.03, Nikon, Tokyo, Japan) was used. Recording of the images for the analysis was obtained with a computer-based system in combination with a DS-Fi1 digital camera, an Eclipse 80i histological microscope (Nikon, Tokyo, Japan) and an automatic scanning table (Prior Scientific, Rockland, MA). With a resolution of 2560 × 1920 pixels and a × 100, a record was made of the area containing the investigated biomaterial as well as the associated peri-implant area assembled from 100 to 200 histological images of interest.

For histomorphometric analysis of the different study parameters, different staining reactions were used as follows: CD31-stained slices were digitized as described above and used to measure the host vascularization within the implantation bed. The blood vessels were marked with the NIS-elements "annotations and measurements" tool and subsequently the number of vessels per square millimeter as well as the vascularization percentage was calculated.

Giant cell activity was analyzed after digitalization of the TRAP-stained sections by counting the number of TRAP-negative multinucleated giant cells as well as TRAP-positive osteoclast-like cells with the NIS-elements software. Thereafter, all unstained and stained multinucleated cells were counted manually and calculated in relation to the total implantation area on 1 mm^2.

Statistical analysis

The histomorphometric data were statistically determined by analysis of variance followed by least significant difference *post-hoc* assessment to compare groups using SPSS 16.0.1 software (SPSS Inc., Chicago, IL, USA) and presented as means ± standard deviations. Differences were considered significant if $P < 0.05$ ($*P < 0.05$), and highly significant if < 0.01 ($**P < 0.01$) or 0.001 ($***P < 0.001$). The GraphPad Prism 5.0d software (GraphPad Software Inc., La Jolla, USA) was used for plotting graphs.

RESULTS

Evaluation of material microstructure and composition

Results of microscopic evaluation of the blanks

The granules showed a crystalline microstructure without indication of tissue or cellular elements between the granules or within granule's interior spaces [Figure 1a and b]. Moreover, no remnants of osteocytic cells were detectable within the lacunae of the matrix [Figure 1b].

In vivo results

All experimental animals survived the surgical procedures without any postoperative complications. No signs of necrosis or severe inflammatory responses were observed at any of the study time points. Detailed description of the tissue reactions toward

the implanted bone substitute material as well as the control operations are described separately below.

Qualitative histopathological results

Tissue reaction of the sham-operated animals

The control wounds healed without complications, and none of the animals showed any signs of severe inflammatory response at the study time points. The histological study revealed high amounts of mononuclear cells that is, macrophages, lymphocytes, (eosinophilic) granulocytes and fibroblasts, within the implantation area at day 3 after implantation (data not shown). Therefore, the amount of cells within this area was visibly higher compared to unaffected areas of subcutaneous connective tissue. Within the time course of the study and the process of wound healing the number of cells decreased, and a regular distribution of cells and extracellular matrix was attained at day 30 after implantation. No multinucleated giant cells were observed at any of the analyzed study time points.

Tissue reaction of the Bio-Oss study group

At day 3 after implantation, qualitative analysis showed that the implantation bed could be divided into an inner core of larger Bio-Oss™ granules and an outer region of small granules or fragments. All these were integrated within a loose network of fibrin and single matrix fibers, while only a marginal invasion of mononucelar cells that is, mainly cells of the monocyte/macrophage line and a few fibroblasts, granulocytes and mast cells, were observable [Figure 2]. The peri-implant tissue showed signs of mild acute inflammation within a cell- and vessel-rich marginal area [Figure 2a]. At this time, point no TRAP-positive cells and no signs of multinucleated giant cells were detectable.

At days 10 and 15 after implantation the BO granules were embedded within a connective tissue that showed minimal signs of inflammation, that is, low numbers of mononuclear cells such as cells of the monocyte/macrophage line, lymphocytes, and granulocytes [Figures 3a and 4a]. Again, the bigger granules of BO were located within the center of the implants and a margin area was detectable, which contained the small material fragments [Figures 3b and 4b]. At the surfaces of the bigger granules mainly mononuclear cells of the monocyte/macrophage line and only a low amount of multinuclear giant cells were seen [Figures 3a and c as well as 4a and c]. Both, the mononuclear and the multinuclear cells showed signs of TRAP expression [Figures 3c and 4c]. In contrast, the small fragments within the margin area of the implants were surrounded by a high number of multinucleated giant cells that mainly showed TRAP expression at this time point, while only a low extent of mononuclear cells was observed [Figures 3b and d as well as 4b and d]. In addition, a moderate vascularization of the intergranular connective tissue was observable, while most of the vessels of the implantation beds were detected at these study time points [Figures 3a and 4a].

The histological analysis revealed additionally that at day 30 up to day 60 after implantation, the granules of the bone substitute remained within the implantation beds, while the small material fragments were no longer locatable [Figures 5a and 6a]. Only a few multinucleated giant cells were detectable on the surfaces of the BO granules, and most of the material-adherent cells were mononuclear cells [Figures 5a and b as well as 6a and b]. The analysis of TRAP expression showed that the few giant cells present were mostly characterized by the expression of this molecule [Figures 5c and 6c]. Only a low amount of the mononuclear cells that were related to the material granules were TRAP-positive, while most of these cells did not show an expression of the TRAP molecule [Figures 5c and 6c]. Furthermore, the above-described mild vascularization of the implantation beds was also observed at these study time points without visible differences compared to the early time points of the study [Figures 5a and 6a].

Quantitative histomorphometrical results

Vessel density

At day 3 after implantation no vessels were detectable within the implantation beds of the study group, while the control group showed a vessel density of 7.94 ± 1.95 vessels/mm^2 [Figure 7a]. However, no significant difference existed between the two groups. Starting at day 10 to day 60 after implantation, the vessel density of the BO group was significantly higher compared with the control group (**$P < 0.01$/***$P < 0.001$) [Figure 7a]. The intra-individual statistical analysis revealed that only between days 3 and 10 after implantation was a significant difference within the BO groups (•••$P < 0.001$) observed, while at the other time points the values of the vessel density remained stable within both study groups [Figure 7a].

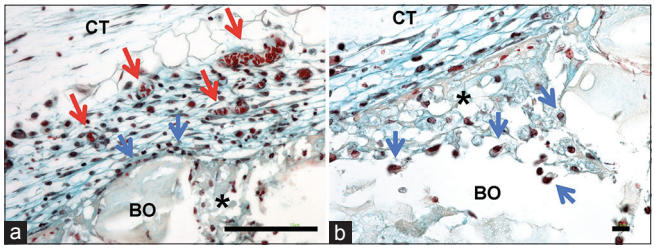

Figure 1: The tissue reaction to the xenogeneic bone substitute Bio-Oss™ at day 3 after implantation. The peri-implant tissue (CT) of the granules (BO) was characterized by a high number of vessels (a, black arrows) and mononuclear cells, that interact with material's surfaces within the periphery of the implantation bed (a and b, blue arrows). Within the interspaces of the granules a matrix composed of connective tissue fibers and fibrin can be observed (a and b, black asterisks) (Movat Pentachrome-stainings, a: ×200, scale bar = 100 μm, b: ×400, scale bar = 10 μm)

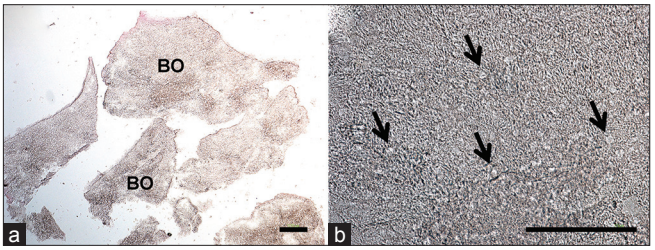

Figure 2: The results of the material characteristics of the xenogeneic bone substitute Bio-Oss™ (BO). (a) The bone substitute shows trabecular architecture without any signs of a lamellar substructure, while the bone matrix appeared crystalline and inhomogeneous. Furthermore, no signs of any other tissue components were identifiable (Giemsa-staining, ×100, scale bar = 100 μm). (b) Within the bone matrix osteocyte lacunae (arrows) without any cells or cell remnants were found (Giemsa-staining, ×400, scale bar = 100 μm)

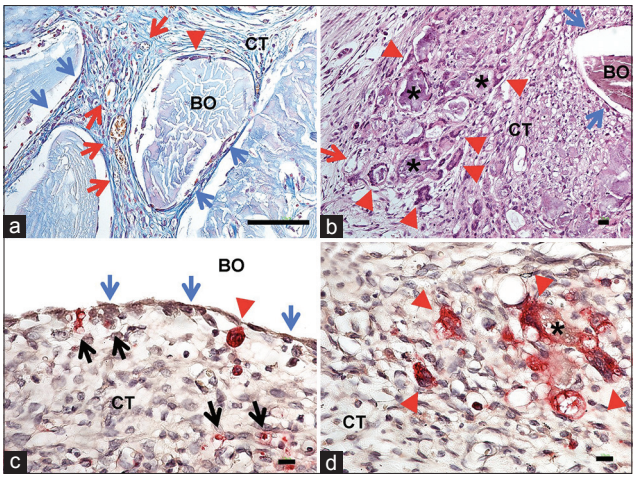

Figure 3: The tissue reaction to the xenogeneic bone substitute Bio-Oss™ at day 10 after implantation. (a) The bigger Bio-Oss™ (BO) granules within the center of the implantation bed were surrounded by a vessel-(black arrows) and fiber-rich connective tissue (CT). At the granule's surfaces mainly mononuclear cells (blue arrows) beside some scattered multinucleated giant cells (blue arrow heads) were observable (Azan-staining, ×100, scale bar = 100 μm). (b) In contrast to the bigger granules (BO), which induced a tissue reaction with mainly mononuclear cells (blue arrows), the smaller granules (green asterisks) within the peripheral regions of the implantation bed were mainly surrounded by high numbers of multinucleated giant cells (blue arrow heads) and integrated within an vessel-rich (black arrows) connective tissue (H and E, ×200, scale bar = 10 μm). (c) Tartrate-resistant acid phosphatase (TRAP)-staining showed that the highest number of mononuclear cells adherent to the larger material granules (BO) were TRAP-negative (blue arrows), while only a few of these cells showed TRAP-expression (red arrows). Moreover, some of the multinucleated giant cells (red arrow heads) did express this molecule, while most of these cells were TRAP-negative (blue arrow heads) (TRAP-staining, ×400, scale bar = 10 μm). (d) The majority of the multinucleated giant cells (red arrow heads) that surrounded the smaller bone substitute granules (green asterisks) showed TRAP-expression as well as many of the mononuclear cells (red arrows) (TRAP-staining, ×400, scale bar = 10 μm)

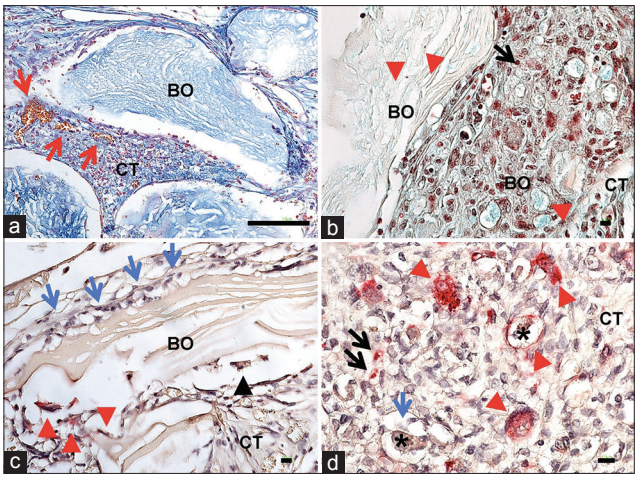

Figure 4: The tissue reaction to the xenogeneic bone substitute Bio-Oss™ at day 15 after implantation. (a) Also, at this time point, the bigger-sized granules (BO) were surrounded by a cell-rich connective tissue (CT), which contained numerous vessels (black arrows). Mainly mononuclear cells (blue arrows) in addition to some single multinucleated giant cells (blue arrow heads) were seen at the surface of the granules (Azan-staining, ×100, scale bar = 100 μm). (b) The small granules of Bio-Oss™ (green asterisks) at this study time point were also embedded within a vessel-(black arrows) and cell-rich connective tissue (CT) and at their surfaces the multinucleated giant cells (blue arrow heads) were still dominant (Movat Pentachrome-staining, ×200, scale bar = 10 μm). (c) The bigger granules were still surrounded by high numbers of tartrate-resistant acid phosphatase (TRAP)-negative mononuclear cells (blue arrows), while only a low amount of these cells were TRAP-positive (red arrows). The majority of the giant cells also showed no signs of TRAP-expression (blue arrow heads) and only single TRAP-positive multinuclear cells were present (red arrow head) (CT = connective tissue) (TRAP-staining, ×200, scale bar = 10 μm). (d) The analysis showed again that most of the giant cells that were adjacent to the smaller material granules (green asterisks) were TRAP-positive (red arrow heads). In addition, TRAP-positive (red arrows) and TRAP-negative mono-nuclear cells (blue arrows) were observed within the implantation bed (TRAP-staining, ×400, scale bar = 10 μm)

Percent vascularization

At day 3 after implantation no vessels were detectable within the implantation beds of the material group, while the control group showed a percent vascularization of 0.06 ± 0.01% [Figure 7b]. No significant difference was measurable in comparison to the BO group. As detected for vessel density analysis, the percent vascularization values of the BO group were significantly higher compared to the values of the control group starting from day 10 to day 60 after implantation (**$P < 0.01$/***$P < 0.001$) [Figure 7b]. Furthermore, an intra-individual significant difference was measurable within the BO groups between days 3 and 10 after implantation (***$P < 0.001$), while the values of the percentage vascularization of both study groups remained at a constant level at the other study time points [Figure 7b].

Material-adherent multinucleated giant cells

At day 3 after implantation no bone substitute material-induced multinucleated giant cells were observable [Figure 7c]. At day 10 after implantation, the extent of multinucleated giant cells (37.09 ± 4.84 cells/mm^2) and their sub forms, that is, TRAP-negative and TRAP-positive giant cells, were significantly increased compared to day 3 (***$P < 0.001$) [Figure 7c]. At this study time point also a significant difference between the extents of the TRAP-negative and TRAP-positive giant cells was measurable (13.16 ± 1.33 vs. 23.93 ± 3.52 cells/mm^2; ***$P < 0.001$) [Figure 7c]. However, from day 15 until the end of the study at day 60 after implantation, no significant differences between the values of TRAP-negative and TRAP-positive giant cells were measurable. However, the values of the total number as well as the amounts of the sub forms significantly increased compared to day 10 after implantation (*$P < 0.1$/***$P < 0.001$) [Figure 7c]. A further increase of the total number of multinucleated giant cells (16.05 ± 3.28 vs. 4.41 ± 1.72 cells/mm^2) as well as of the TRAP-negative giant cells (9.52 ± 2.02 vs. 2.68 ± 0.91 cells/mm^2) was measured between day 15 and day 30 after implantation (*$P < 0.1$/***$P < 0.001$), while the number of TRAP-positive giant cells remained stable (6.52 ± 1.27 vs. 1.73 ± 0.82 cells/mm^2) [Figure 7c]. No intra-individual significant differences were measured between days 30 and 60 after implantation within all three groups.

DISCUSSION

The biomaterial world has witnessed an influx of numerous bone graft materials and their synthetic substitutes within the past few decades, each attempting to match the qualities of autogenous

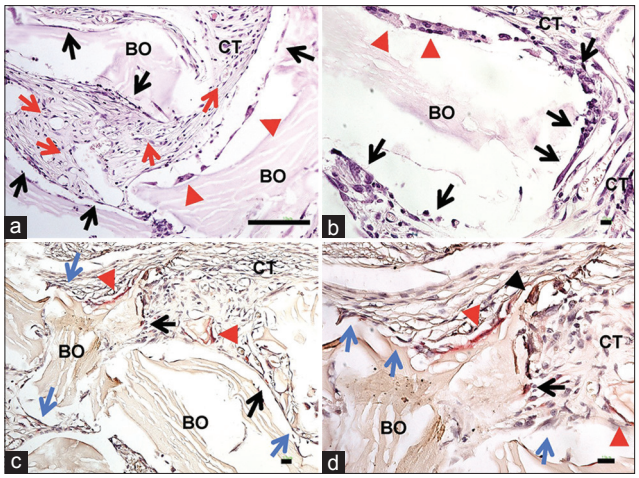

Figure 5: The tissue reaction to the xenogeneic bone substitute Bio-OssTM at day 30 after implantation. (a and b) The Bio-OssTM granules (BO) were still embedded within a fiber-rich connective tissue (CT) associated with numerous blood vessels (black arrows). Mainly mononuclear cells (blue arrows) and also a few giant cells (blue arrow heads) were still observable at the material surfaces at this time point (H and E, a: ×100, scale bar = 100 μm; b: ×200, scale bar = 10 μm). (c and d) The mononuclear cells were mainly tartrate-resistant acid phosphatase (TRAP)-negative (blue arrows) and only single cells were identifiable expressing the TRAP-molecule (black arrows). At this time point, the multinuclear cells also show mainly TRAP-positivity (red arrow heads) (TRAP-negative giant cells = black arrow heads) (BO = Bio-Oss granules) (TRAP-staining, c: ×100; d: ×400, scale bars = 10 μm)

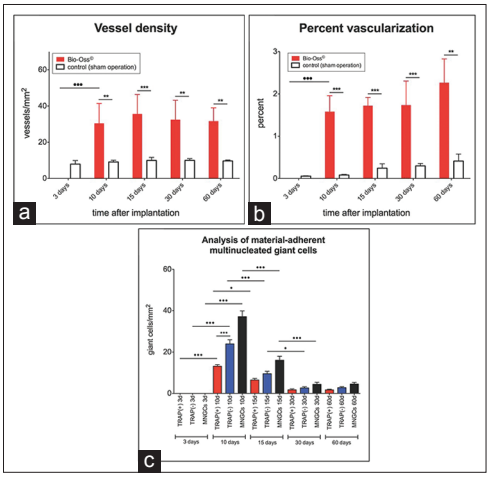

Figure 7: The histomorphometrical results. (a) Vessel density (vessels/mm^2), (b) Percent vascularization (% area of vessels/area of implantation bed), (c) Multinucleated giant cells and their tartrate-resistant acid phosphatase (TRAP)-positive and TRAP negative subforms (cells/mm^2)

bone grafts. Deproteinized bovine bone graft, Bio-Oss™ is an example of these materials, which has been shown to be closely related to autografts because of its biocompatibility, and efficacy in bony augmentations.[6-9] It is important to note that the assessment of the effectiveness of a good bone graft material should be made by its ability to remain in the implantation bed and to maintain space for tissue regeneration.[11] These qualities have been demonstrated by Bio-Oss™ as the material has been seen in the augmentation beds years after implantation.[7,9,11] Fast absorption and degradation in the augmentation bed may jeopardize repair as a result of failure of newly formed bone to replace the degraded biomaterial by the process of creeping substitution.[14,22]

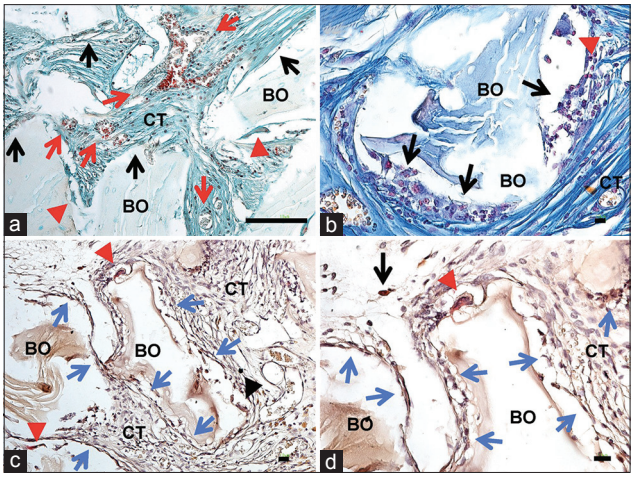

Figure 6: The tissue reaction to the xenogeneic bone substitute Bio-OssTM at day 60 after implantation. (a and b) The intergranular connective tissue (CT) of the Bio-OssTM granules (BO) still showed a fiber-and vessel-rich (black arrows) composition. Also, at this time point most of the adherent cells were mononuclear (blue arrows) and only a minority of the reacting cells was multinuclear (blue arrow heads) (a: Masson Goldner-staining, ×100, scale bar = 100 μm; b: Azan-staining, ×400, scale bar = 10 μm). (c and d) The single multinucleated giant cells mainly showed tartrate-resistant acid phosphatase (TRAP)-expression (red arrow heads) at this time point, while only single TRAP-negative multinucleated cells (black arrow head) were found. The majority of the mononuclear cells were TRAP-negative (blue arrows). Only single TRAP-positive mononuclear cells (black arrow) were observable at this time point (TRAP-staining, c: ×100, ; d: ×400, scale bars = 10 μm

In this study, among other parameters, we analyzed the participating cells and the cellular mechanisms taking place in the initial integration and degradation process of Bio-Oss™ following implantation in a well-established subcutaneous implantation model of CD1 mice. As early as the 3rd day postimplantation, mild signs of acute inflammation were recorded in the peri-implant tissue with a marginal invasion of mononuclear cells, but no TRAP-positive cells or multinucleated giant cells were detected. This was similar to the findings of Tapety *et al*.[11] in which they also observed early cellular migration around the implanted biomaterial at day 3 of their study, but these cells did not exhibit alkaline phosphatase or TRAP.

A significant finding from our study, however, was the granular arrangement of Bio-Oss (BO) particles following implantation. The smaller fragments of the biomaterial as seen at days 10 and 15 of the study attracted more mononucleated and multinucleated giant cells which showed signs of TRAP expression than the centrally located larger granules.

There was also evidence of intergranular connective tissue vascularization with most of the vessels in the implantation bed evident at this stage of the study. Interestingly, at days 30 and 60 of the study period, these small fragments were no longer seen in the implantation bed and only a few multinucleated giant cells were present. It is assumed that these small fragments of the biomaterials were responsible for the early induction of a cellular reaction and vascularization, which is necessary for successful integration of the biomaterial into the surrounding tissue.

It has been previously demonstrated that changes in size, porosity and shape of biomaterials can be used to regulate the extent of

the immunological reaction of the host tissue, which in turn can contribute to the degree of formation of multinucleated giant cells, thus influencing material vascularization and degradation.[14] The composition of the bone-substitute material can be used to tailor its stability.

This may indeed explain the result that was documented by Piattelli *et al*.[7] in their histological analysis of bone reaction to BO used in human sinus augmentations. They reported that the BO particles were surrounded in all cases by an abundant quantity of newly formed lamellar bone while still maintaining the inner core of the biomaterial after 4 years of implantation. BO tends to promote more early bone formation than other bone substitutes,[23] while simultaneously undergoing a very slow resorption.[24] The particles are assumed to act as resorbable osteoconductive scaffolds along which new bone tissue can form.[5,24]

The onset and rate of degradation of a biomaterial are important, as they affect the biologic response to the material.[9,25-27] Bio-Oss™, in this study, tended to induce an early cellular reaction and vascularization. Simultaneously, it underwent a slow degradation, because the bigger central granules attracted only a few multinuclear giant cells. This gives the biomaterial a kind of stability over time in the implantation bed and this property is a prerequisite for the augmentation of bony defects and the support of implant stability over a long period of time.

This idea however was not shared by Schlegel *et al*.[9] who postulated that Bio-Oss™ is not resorbed at all following implantation. They reported that their histological analysis after about 6 months of implantation did not reveal any signs of Bio-Oss™ resorption, claiming that the initial reduction in volume of the biomaterial could be explained rather by shrinkage than by resorption. Our study on the other hand revealed a significant presence of multinucleated giant cells and their sub-form, that is, TRAP-positive and TRAP-negative giant cells, from day 10 to about day 30 of the study period. At day 10 after implantation, the extent of multinucleated giant cells and their sub forms were significantly increased compared to day 3. Moreover, at this study time point a measurable significant difference was observed between TRAP-negative and TRAP-positive giant cells. Furthermore, from day 15 until the end of the study at day 60 after implantation, no significant differences were observed regarding the number of TRAP-negative and TRAP-positive giant cells.

The number of multinucleated giant cells at the implantation bed varies depending on the physicochemical structure of the biomaterials, and they are thought to be responsible for the degradation of the bone substitute materials. At the same time, they induce vascularization by releasing VEGF and other chemokines.[3,10] They can also produce acid phosphatases and osteoclast-specific cell markers, which has led to the term "osteoclast-like cells".[28,29] These enzymes determine the biodegradability of a biomaterial.[30] In this study, there was a significant presence of these osteoclast-like cells (TRAP cells), starting from day 10 of our study, which further supports the biodegradability of Bio-Oss™.

What remains to be understood however, is the nature of these multinucleated cells, that is, whether they are osteoclasts or FBGCs, bearing in mind that FBGC do not necessarily exhibit osteoclast markers such as TRAP, calcitonin receptor, or receptor activator of nuclear factor κB.[31] Further studies are also needed to investigate if these cells are really necessary for successful biomaterial integration.

CONCLUSIONS

This study analyzed the host cellular reactions to the bovine bone substitute material Bio-Oss™, following implantation in a well-established subcutaneous implantation model in CD1 mice. In the early stages of implantation, the smaller granules of the biomaterial were seen to attract more mono- and multi-nucleated giant cells, which showed increased signs of TRAP expression, compared to the central bigger granules. It is however still not clear from this study, what the true nature of these multinucleated giant cells is, whether they are osteoclasts or FBGC.

There was also evidence for intergranular connective tissue vascularization with most of the vessels in the implantation bed, present at the early stage of the study. These smaller granules were no longer seen at the end of the study period, leaving only the larger BO granules and a few multinucleated giant cells. It is therefore assumed that the small fragments of the biomaterials were responsible for the early induction of a cellular reaction and vascularization, which is necessary for a successful integration of the biomaterial into the surrounding tissue. This result could help explaining, why BO can be observed in its implantation bed long after implantation. This also means that BO is very suitable for clinical application in various forms of bony augmentations, such as sinus lift and guided bone regeneration.

ACKNOWLEDGMENTS

The authors would like to thank Mrs. Ulrike Hilbig and Mr. Mykhaelo Reshetnykov for their excellent technical assistance. This research was funded by the research funds of the authors.

REFERENCES

1. Figueiredo A, Silva O, Cabrita S. Inflammatory reaction post implantation of bone grafts materials. Exp Pathol Health Sci 2012;6:15-8.
2. Moore WR, Graves SE, Bain GI. Synthetic bone graft substitutes. ANZ J Surg 2001;71:354-61.
3. Ghanaati S, Udeabor SE, Barbeck M, Willershausen I, Kuenzel O, Sader RA, *et al*. Implantation of silicon dioxide-based nanocrystalline hydroxyapatite and pure phase beta-tricalciumphosphate bone substitute granules in caprine muscle tissue does not induce new bone formation. Head Face Med 2013;9:1.
4. Kurz LT, Garfin SR, Booth RE Jr. Harvesting autogenous iliac bone grafts. A review of complications and techniques. Spine (Phila Pa 1976) 1989;14:1324-31.
5. Hürzeler MB, Quiñones CR, Kirsch A, Gloker C, Schüpbach P, Strub JR, *et al*. Maxillary sinus augmentation using different grafting materials and dental implants in monkeys. Part I. Evaluation of anorganic bovine-derived bone matrix. Clin Oral Implants Res 1997;8:476-86.
6. Valentini P, Abensur D, Densari D, Graziani JN, Hämmerle C. Histological evaluation of Bio-Oss in a 2-stage sinus floor elevation and implantation procedure. A human case report. Clin Oral Implants Res 1998;9:59-64.
7. Piattelli M, Favero GA, Scarano A, Orsini G, Piattelli A. Bone reactions to anorganic bovine bone (Bio-Oss) used in sinus augmentation procedures: A histologic long-term report of 20 cases in humans. Int J Oral Maxillofac

Implants 1999;14:835-40.
8. Lorenzetti M, Mozzati M, Campanino PP, Valente G. Bone augmentation of the inferior floor of the maxillary sinus with autogenous bone or composite bone grafts: A histologic-histomorphometric preliminary report. Int J Oral Maxillofac Implants 1998;13:69-76.
9. Schlegel KA, Fichtner G, Schultze-Mosgau S, Wiltfang J. Histologic findings in sinus augmentation with autogenous bone chips versus a bovine bone substitute. Int J Oral Maxillofac Implants 2003;18:53-8.
10. Ghanaati S, Barbeck M, Detsch R, Deisinger U, Hilbig U, Rausch V, *et al*. The chemical composition of synthetic bone substitutes influences tissue reactions *in vivo*: Histological and histomorphometrical analysis of the cellular inflammatory response to hydroxyapatite, beta-tricalcium phosphate and biphasic calcium phosphate ceramics. Biomed Mater 2012;7:015005.
11. Tapety FI, Amizuka N, Uoshima K, Nomura S, Maeda T. A histological evaluation of the involvement of Bio-Oss in osteoblastic differentiation and matrix synthesis. Clin Oral Implants Res 2004;15:315-24.
12. Oliveira R, El Hage M, Carrel JP, Lombardi T, Bernard JP. Rehabilitation of the edentulous posterior maxilla after sinus floor elevation using deproteinized bovine bone: A 9-year clinical study. Implant Dent 2012;21:422-6.
13. Ghanaati S, Orth C, Barbeck M, Willershausen I, Thimm BW, Booms P, *et al*. Histological and histomorphometrical analysis of a silica matrix embedded nanocrystalline hydroxyapatite bone substitute using the subcutaneous implantation model in Wistar rats. Biomed Mater 2010;5:035005.
14. Ghanaati S, Barbeck M, Orth C, Willershausen I, Thimm BW, Hoffmann C, *et al*. Influence of β-tricalcium phosphate granule size and morphology on tissue reaction *in vivo*. Acta Biomater 2010;6:4476-87.
15. Ghanaati S, Barbeck M, Hilbig U, Hoffmann C, Unger RE, Sader RA, *et al*. An injectable bone substitute composed of beta-tricalcium phosphate granules, methylcellulose and hyaluronic acid inhibits connective tissue influx into its implantation bed *in vivo*. Acta Biomater 2011;7:4018-28.
16. Peetz M. Characterization of xenogeneic bone material. In: Boyne PJ, editors. Osseous Reconstruction of the Maxilla and Mandible. Chicago: Quintessence; 1997. p. 87-93.
17. Manufacturing of Geistlich Bio-Oss®. Available from: http://www.geistlich.com/?dom=2 and rub=142. [Last retrieved on 2013 Oct 28].
18. Gross JS. Bone grafting materials for dental applications: A practical guide. Compend Contin Educ Dent 1997;18:1013-8, 1020.
19. Benke D, Olah A, Möhler H. Protein-chemical analysis of Bio-Oss bone substitute and evidence on its carbonate content. Biomaterials 2001;22:1005-12.
20. Figueiredo M, Henriques J, Martins G, Guerra F, Judas F, Figueiredo H. Physicochemical characterization of biomaterials commonly used in dentistry as bone substitutes – Comparison with human bone. J Biomed Mater Res B Appl Biomater 2010;92:409-19.
21. Ghanaati S, Unger RE, Webber MJ, Barbeck M, Orth C, Kirkpatrick JA, *et al*. Scaffold vascularization *in vivo* driven by primary human osteoblasts in concert with host inflammatory cells. Biomaterials 2011;32:8150-60.
22. Accorsi-Mendonça T, Conz MB, Barros TC, de Sena LA, Soares Gde A, Granjeiro JM. Physicochemical characterization of two deproteinized bovine xenografts. Braz Oral Res 2008;22:5-10.
23. Klinge B, Alberius P, Isaksson S, Jönsson J. Osseous response to implanted natural bone mineral and synthetic hydroxylapatite ceramic in the repair of experimental skull bone defects. J Oral Maxillofac Surg 1992;50:241-9.
24. Wetzel AC, Stich H, Caffesse RG. Bone apposition onto oral implants in the sinus area filled with different grafting materials. A histological study in beagle dogs. Clin Oral Implants Res 1995;6:155-63.
25. Burg KJ, Porter S, Kellam JF. Biomaterial developments for bone tissue engineering. Biomaterials 2000;21:2347-59.
26. Houser BE, Mellonig JT, Brunsvold MA, Cochran DL, Meffert RM, Alder ME. Clinical evaluation of anorganic bovine bone xenograft with a bioabsorbable collagen barrier in the treatment of molar furcation defects. Int J Periodontics Restorative Dent 2001;21:161-9.
27. Yamada S, Shima N, Kitamura H, Sugito H. Effect of porous xenographic bone graft with collagen barrier membrane on periodontal regeneration. Int J Periodontics Restorative Dent 2002;22:389-97.
28. Kadoya Y, al-Saffar N, Kobayashi A, Revell PA. The expression of osteoclast markers on foreign body giant cells. Bone Miner 1994;27:85-96.
29. Ibbotson KJ, Roodman GD, McManus LM, Mundy GR. Identification and characterization of osteoclast-like cells and their progenitors in cultures of feline marrow mononuclear cells. J Cell Biol 1984;99:471-80.
30. Detsch R, Mayr H, Ziegler G. Formation of osteoclast-like cells on HA and TCP ceramics. Acta Biomater 2008;4:139-48.
31. McNally AK, Anderson JM. Foreign body-type multinucleated giant cells induced by interleukin-4 express select lymphocyte co-stimulatory molecules and are phenotypically distinct from osteoclasts and dendritic cells. Exp Mol Pathol 2011;91:673-81.

Cite this article as: Barbeck M, Udeabor SE, Lorenz J, Kubesch A, Choukroun J, Sader RA, *et al*. Induction of multinucleated giant cells in response to small sized bovine bone substitute (Bio-Oss ™) results in an enhanced early implantation bed vascularization. Ann Maxillofac Surg 2014;4:150-7.

Source of Support: Nil, **Conflict of Interest**: None declared.